Theoretical Analysis of the Bonding between CO and Positively Charged Atoms

Anthony J. Lupinetti,[†,‡] Stefan Fau,[†] Gernot Frenking,*[,†] and Steven H. Strauss*[,‡]

Fachbereich Chemie, Philipps-Universität Marburg, Hans-Meerwein-Strasse, D-35032 Marburg, Germany, and the Department of Chemistry, Colorado State University, Fort Collins, Colorado 80523

Received: August 23, 1997[⊗]

A detailed analysis of the changes in the electronic structure of CO when a proton or a positive charge approaches the carbon or the oxygen atom is reported using quantum mechanical ab initio calculations and several methods to analyze the theoretical data. The C−O bond is shortened by nearly the same amount in HCO^+ and QCO^+ compared to free CO, while the nearly identical C−O bond lengths of COH^+ and COQ^+ are longer than in CO. H^+ and Q^+ have a strong electrostatic effect upon the atom to which they are bonded, which leads to an increased electronegativity of carbon and oxygen, respectively. Inspection of the charge distribution and the natural localized orbitals shows clearly that the shorter C−O distances of HCO^+ and QCO^+ and the longer C−O bond lengths of COH^+ and COQ^+ are due to the changes in the polarization of the bonding orbitals which are caused by the positive charge of H^+ or Q^+ that are bonded to the molecule. The bonding orbitals of CO are polarized toward the more electronegative oxygen end. A proton or a positive charge at carbon attracts electronic charge from the oxygen atom toward the carbon end, which leads to less polarized σ- and π-bonds and to a more covalent C−O bond. A positive charge or a proton at the oxygen atom has the opposite effect. The calculated curve of the C−O bond length in MCO^+ (M = Li, Cu, Ag, Au) as a function of the M^+−CO distance shows that the C−O bond becomes shorter in the beginning when the metal cation approaches the carbon atom. There is a turning point at shorter M^+−CO distances where the C−O bond becomes longer again. The charge decomposition analysis shows that the position of the turning point is determined by the onset of the metal$^+$ → CO back-donation. A relatively small amount of M^+ → CO back-donation is sufficient to lengthen the CO bond. The turning point for the curve of the C−O bond length as a function of the M^+−CO distance occurs at a M^+−CO value that is shorter than the equilibrium distance for M = Li and Ag, while it is longer for M = Cu and Au. The trends of the bond strengths and M^+−CO interactions are explained with the radii and orbital energies of the valence *n*s and (*n* − 1)d orbitals of the transition metals.

Introduction

The classical picture of metal−ligand bonding in transition metal carbonyl complexes given in textbooks of inorganic and transition metal chemistry describes the donor−acceptor bonds in terms of synergistic bonding, where carbon monoxide acts simultaneously as σ-donor and π-acceptor (Chart 1).[1] Theoretical studies about the nature of the metal−CO bond have shown[2−4] that the dominant orbital interactions at CO involve the HOMO, which has its major extension at the carbon end (σ donation) and the C−O antibonding LUMO (π-back-donation). There is general agreement now that for most transition metal carbonyl complexes the metal → CO π-back-donation is more important for the bonding energy than the OC → metal σ-donation,[2] although the amount of σ-donation is higher than that of π-back-donation.[4] The reason is that the HOMO of CO encounters significant electron repulsion with occupied orbitals of the metal, which counterbalances the bonding interactions of the CO donor orbital with empty orbitals at the metal.[2] Electron donation from the occupied π orbital of CO to the metal, which has been suggested as additional source of metal−CO bonding interactions,[1a] was found to be insignificant.[4]

The picture described above is valid for "classical" carbonyl complexes, which are clearly the majority of the metal carbonyls. There is an increasing number of stable carbonyl complexes for which the metal → CO π-back-donation is *not* important, and where the dominant bonding interactions are due to OC → metal σ donation.[5−7] This class of metal carbonyls has been termed "nonclassical".[6] Many nonclassical carbonyl complexes are positively charged species, e.g. $M(CO)^+$ and $M(CO)_2^+$ (M = Cu, Ag, Au) or the recently reported $Ir(CO)_6^{3+}$.[7] Theoretical studies of these cations have shown that metal → CO π-back-donation is indeed negligible and that the bonding is mainly due to OC → metal σ donation besides electrostatic attraction.[4a,8] The OC → metal σ interaction is bonding at longer distances, because the empty metal orbitals are more diffuse than the occupied orbitals. This is particularly true when the metal is positively charged. Highly charged metal carbonyls may have strong bonds in spite of having little metal → CO π-back-donation, because the acceptor orbitals at the metal are energetically low lying and the additional Coulomb attraction is rather strong.[8a]

CHART 1: Schematic Representation of the Metal−CO Donor−Acceptor Interactions in Terms of OC → M σ Donation and M → CO π-Back-donation

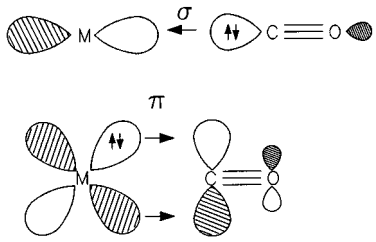

It is tempting to classify a carbonyl complex as classical or nonclassical by the frequency of the C−O stretching mode: classical metal carbonyls have υ(CO) < 2143 cm^{-1}, and

[†] Philipps-Universität Marburg.
[‡] Colorado State University.
[⊗] Abstract published in *Advance ACS Abstracts,* November 15, 1997.

S1089-5639(97)02657-1 CCC: $14.00

CHART 2: Schematic Representation of the Change in the C−O Bond Length and Stretching Frequency υ(CO) along the M−CO Coordinate

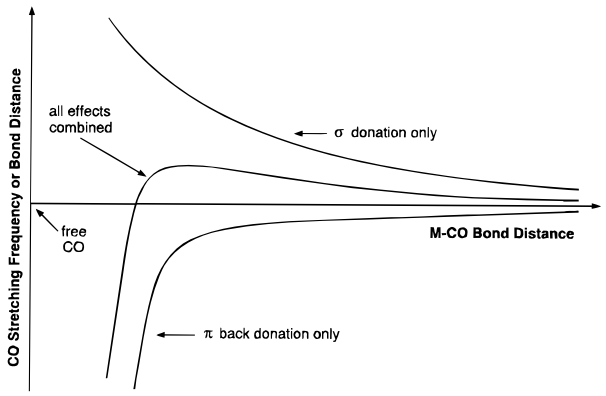

nonclassical metal carbonyls have υ(CO) > 2143 cm^{-1}. However, while the C−O stretching frequency increases first when a metal cation approaches CO until it reaches a maximum, there might be significant metal → CO π-back-donation before the C−O stretching mode becomes <2143 cm^{-1} again. This is shown schematically in Chart 2. It follows that classical carbonyls may also have C−O stretching frequencies which are greater than 2143 cm^{-1}. A more detailed discussion of the difference between classical and nonclassical carbonyls is found elsewhere.[9]

This work is concerned with two aspects of the bonding in carbonyl compounds. One aspect is the reason for the increase in the C−O stretching frequency in carbonyl compounds where σ donation is the dominant factor for the bonding interactions, i.e., in *nonclassical* carbonyls. The standard textbook explanation states that the HOMO of CO is *antibonding* in the interatomic region.[10] The explanation was first given by Fenske et al.,[11] who showed that the Mulliken population analysis of approximate molecular orbitals is antibonding for the HOMO. This finding gave a plausible reason for the experimental result that for CO^+ the vibrational frequency (2184 cm^{-1}) and the force constant (19.26 mdyn/Å) are higher than that of CO (2143 cm^{-1} and 18.56 mdyn/Å) and that CO^+ has a shorter equilibrium distance (1.1150 Å) than CO (1.1331 Å).[12] Another experimental result which could be explained by assuming an antibonding HOMO for CO was the finding that HCO^+ has also a higher C−O stretching frequency (2184 cm^{-1}), a larger C−O force constant (21.3 mdyn/Å),[13] and a shorter C−O distance (1.1047 Å) than CO.[14]

There is an important theoretical result, however, which speaks against the suggestion that the HOMO of CO is antibonding. Ab initio calculations at the Hartree−Fock level of theory give a HOMO which is highly localized at the carbon end, but it is *bonding* between carbon and oxygen. This result is independent of the quality of the basis set. Calculations at the same level of theory predict that CO^+ and HCO^+ have *higher* C−O vibrational frequencies than CO, although the HOMO of CO is bonding. There must be another factor besides the nature of the HOMO which influences strongly the C−O interactions.

The second aspect of carbonyl bonding discussed in this work is concerned with the relationship between the two components σ-donation and π-back-donation in metal carbonyl cations M^+−CO and the influence of the two different types of interactions upon the C−O bond length.

In this paper we report results of a theoretical study which show that the major reason which leads to a change in the C−O stretching frequency, the associated force constant, and the equilibrium distance of XCO^+ and COX^+, is in the absence of strong π interactions the electrostatic effect of X^+ upon CO. This explains why the C−O frequency and force constant *decrease* when X^+ approaches CO from the oxygen end, while they *increase* when X^+ approaches from the carbon end. A similar conclusion has been reached in an independent theoretical study by Goldman and Krogh-Jespersen,[15] who showed that a positive point charge Q^+ at the carbon end of CO has nearly the same effect as a proton. Our work complements the important work of these authors by showing the results not only for QCO^+ but also for COQ^+ together with an analysis of the changes in the electronic structure of CO when Q^+ approaches CO from the oxygen or the carbon end. The results are compared with calculated data for HCO^+ and COH^+. It becomes clear that the electrostatic effect of the proton upon CO, which was suggested by Goldmann and Krogh-Jespersen to be the main reason for the bond shortening and increase of the force constant, operates indirectly by reducing the polarity of the C−O bond orbitals. Further theoretical results are reported for $M(CO)^+$ (M = Li, Cu, Ag, Au). It is shown that the C−O distance decreases first when CO approaches a positively charged metal. The curve of the C−O bond length as a function of the M^+−CO distance has a turning point, at which r_{CO} becomes longer. The turning point may be at a longer or shorter distance than the $M(CO)^+$ equilibrium geometry. The onset of the C−O bond lengthening is clearly connected to the extent of M → CO π-back-donation.

Carbonyl cations XCO^+ and COX^+ (X = H, Li, Cu, Ag, Au) have been studied theoretically before, but most studies were concerned with the structure and bond energy of the cations.[16] In a pioneering initial study, Hall and Fenske[17] compared calculated orbital populations taken from approximate calculations with with experimental vibrational frequency data. Beach and Jolly[18] suggested that the rehybridization of the CO 4σ and 5σ orbitals is responsible for the increase of υ(CO) when CO becomes coordinated to BH_3, but the effect of the π orbitals was not considered. This study focuses on the changes of the properties and electronic structure of CO when X^+ becomes attached.

Methods

The geometry optimizations and frequency calculations were carried out at the MP2/6-31G(d,p) level of theory. For Cu, Ag, and Au a quasi-relativistic small-core effective core potential (ECP) of Stoll and Preuss[19] with a (311111/22111/411) valence shell basis set was used. Improved total energies are calculated at the CCSD(T) level[20] using the same basis set at geometries optimized at the MP2 level of theory. The Coulomb effect of a positive point charge Q^+ was achieved in two different ways. One way was by using a proton which has no orbital. This method was chosen for the geometry optimization and the frequency calculations, because it is then possible to use analytical gradients for the geometry optimization. The second way was the use of a true point charge, i.e., a positive charge which has no mass. Both methods were used for the analysis of the electronic structure of QCO^+ and COQ^+. The results were the same. The calculations were carried out using the program package Gaussian 94.[21] The CCSD(T) calculations were performed using the program ACES II.[22] The electronic structure of the compounds was analyzed using the natural bond orbital (NBO) partitioning scheme developed by Weinhold[23] and the topological analysis of the electron density distribution developed by Bader.[24] The relative amounts of OC → M donation and M → CO π-back-donation were calculated using the CDA (charge decomposition analysis) method developed

TABLE 1: Calculated Changes (MP2/6-31G(d)) of HCO^+ and QCO^+ as a Function of the H^+-CO and Q^+-CO Distance[a]

HCO^+					QCO^+				
r_{H^+-C}	r_{C-O}	ν_{CO}	F_{CO}[b]	E_{rel}	r_{Q^+-C}	r_{C-O}	ν_{CO}	F_{CO}[b]	E_{rel}
0.5	1.119	2253	22.44	461.7	0.5	1.115	2255	22.46	511.8
0.75	1.126	2204	21.53	−46.1	0.75	1.121	2252	22.52	20.2
1.0	1.130	2171	21.25	−144.8	1.0	1.127	2163	21.79	−64.2
1.095	1.131	2137	21.16	−149.2	1.095	1.130	2069	21.52	−71.0
1.186	1.131	2031	21.03	−146.3	1.186	1.131	1898	21.31	−72.7
1.5	1.134	2222	20.62	−116.2	1.5	1.136	2249	20.77	−60.6
2.0	1.138	2183	20.12	−67.5	2.0	1.141	2185	20.11	−30.7
2.5	1.140	2168	19.80	−35.9	2.5	1.144	2163	19.67	−15.1
3.0	1.142	2157	19.58	−17.5	3.0	1.146	2152	19.48	−8.4
3.5	1.145	2147	19.38	−8.1	3.5	1.147	2145	19.37	−5.2
4.0	1.147	2141	19.29	−4.1	4.0	1.147	2140	19.31	−3.5
∞	1.151	2125	18.92	0.0	∞	1.151	2125	18.92	0.0

[a] Distances r in Å, frequencies ν in cm^{-1}, force constants F in mdyn/Å, and relative energies E_{rel} in kcal/mol. [b] Calculated using eq 1, see text.

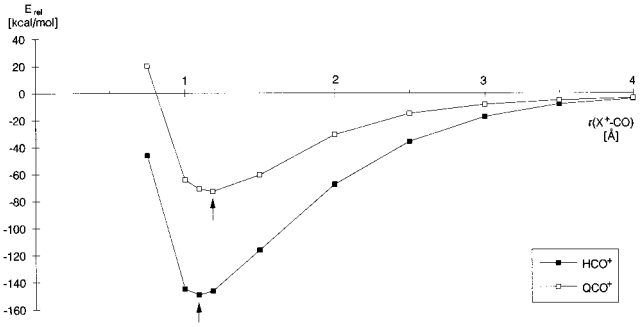

Figure 1. Plot of the calculated energies E_{rel} (kcal/mol) of XCO^+ (X = H^+ or point charge Q^+) at various distances X^+-CO. Arrows show the position of the equilibrium structure.

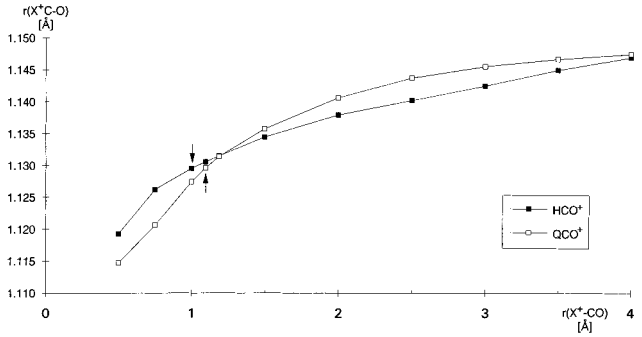

Figure 2. Plot of the calculated C−O distances (Å) of XCO^+ (X = H^+ or point charge Q^+) at various distances X^+-CO. Arrows show the position of the equilibrium structure.

by Dapprich and Frenking.[25] For the topological analysis of the charge distribution the programs BONDER, EXTREM, and SADDLE were employed.[26]

We calculated the internal force constants for the C−O stretching mode F_{CO} using eq 1, which has been suggested by Goldman and Krogh-Jespersen.[9] The F_{CO} values are obtained from the energy changes resulting from extension of the C−O bond length by 0.01 Å relative to the energy minimzed geometries in the carbonyl complex (ΔE_{XCO}) and free CO (ΔE_{CO}):

$$F_{CO} = (\Delta E_{XCO}/\Delta E_{CO})F_{CO} \quad (1)$$

The reference value F_{CO} is the calculated value at MP2/6-31G-(d), i.e., 18.92 mdyn/Å.

Interaction of CO with a Proton H^+ and a Positive Charge Q^+

In order to estimate the difference between the effect of a proton H^+ and a positive charge Q^+ upon the energy, the interatomic distance, and the vibrational mode of CO, we optimized the geometries of linear HCO^+ and QCO^+ and calculated the vibrational frequencies at fixed distances H^+-CO and Q^+-CO using intervals between 4.0 and 0.5 Å. Table 1 shows the calculated results. Figure 1 shows a plot of the calculated energies of HCO^+ and QCO^+ as a function of the H^+-CO and Q^+-CO distances. The energy minimum of HCO^+ is calculated at $r_{H-C} = 1.095$ Å and at $r_{C-O} = 1.131$ Å, which is shorter than the calculated value for free CO (1.151 Å). The shorter C−O bond of HCO^+ compared with free CO is in agreement with the above-cited experimental results and with recent theoretical work at the CCSD(T)/cc-pVQZ level of theory,[27] which gave $r_{H-C} = 1.093$ Å and $r_{C-O} = 1.109$ Å for HCO^+ and 1.131 Å for the bond length of free CO.

The theoretically predicted H^+-CO bond energy is $D_e = 149.2$ kcal/mol, which gives after correcting for zero-point energy contributions (ZPE) a calculated proton affinity of $D_0 = 142.1$ kcal/mol. This is in good agreement with the experimentally observed proton affinity of 141.6 kcal/mol[28] and with a theoretically predicted value at CCSD(T)/cc-pVQZ $D_0 = 140.2$ kcal/mol.[27] Figure 1 shows that the potential energy curve of Q^+-CO has a similar shape as H^+-CO but that the well depth of QCO^+ is not as deep as for HCO^+. The energy minimum is calculated at $r_{Q-C} = 1.186$ Å and $r_{C-O} = 1.131$ Å. The charge stabilization energy of QCO^+ is 72.7 kcal/mol, which is about half of $D_e(H^+-CO) = 149.2$ kcal/mol. It follows that half of the bond energy of the H^+-CO bond is due to electrostatic attraction.

Table 1 shows that the C−O bond lengths r_{CO} of HCO^+ and QCO^+ become shorter when the proton or the charge approaches the carbon end. Figure 2 shows a plot of the C−O distance as a function of r_{H^+-CO} and r_{Q^+-CO}, respectively. The two curves are very similar. In particular, the r_{C-O} bond shortening of HCO^+ at the equilibrium distance ($\Delta r_{CO} = -0.019$ Å) is nearly the same as calculated for QCO^+ using the r_{H^+-CO} equilibrium distance ($\Delta r_{CO} = -0.020$ Å, see Table 1). The results listed in Table 1 and displayed in Figure 2 show clearly that *the C−O bond shortening of HCO^+ is nearly exclusively caused by the electrostatic effect of the positive charge at the proton.*

A very interesting result is given when the change of the C−O distance of HCO^+ and QCO^+ is compared with the change of the stretching frequency ν_{CO} and force constant F_{CO} (Table 1). The frequency and the force constant increase first, when H^+ or Q^+ approaches the carbon atom. This is expected, because the C−O bond distances decreases. At $r_{H-CO} = 1.50$ Å, the C−O frequency has increased by nearly 100 cm^{-1}. However, when the proton or positive charge is close to the carbon atom, the wavenumber of the C−O mode suddenly

TABLE 2: Calculated Changes (MP2/6-31G(d)) of COH^+ and COQ^+ as a Function of the $CO-H^+$ and $CO-Q^+$ Distance[a]

COH^+					COQ^+				
r_{O-H^+}	r_{C-O}	ν_{CO}	F_{CO}[b]	E_{rel}	r_{O-Q^+}	r_{C-O}	ν_{CO}	F_{CO}[b]	E_{rel}
0.5	1.158	2033	17.92	422.0	0.5	1.156	2087	18.89	482.5
0.75	1.166	1994	17.28	−43.1	0.75	1.162	2063	18.56	10.3
1.0	1.168	1973	17.13	−102.3	1.0	1.169	1984	17.42	−49.0
1.007	1.168	1971	17.12	−102.3	1.007	1.169	1982	17.39	−49.2
1.055	1.169	1957	17.11	−101.3	1.055	1.169	1965	17.42	−49.8
1.5	1.169	2005	17.10	−62.3	1.5	1.163	2053	18.00	−30.9
2.0	1.164	2030	17.62	−28.0	2.0	1.158	2084	18.46	−13.6
2.5	1.158	2068	18.21	−11.6	2.5	1.156	2099	18.67	−6.6
3.0	1.155	2096	18.61	−4.9	3.0	1.154	2107	18.77	−3.6
3.5	1.153	2109	18.82	−2.4	3.5	1.153	2111	18.86	−2.2
4.0	1.153	2114	18.88	−1.4	4.0	1.153	2114	18.88	−1.4
∞	1.151	2125	18.92	0.0	∞	1.151	2125	18.92	0.0

[a] Distances r in Å, frequencies ν in cm^{-1}, force constants F in mdyn/Å, and relative energies F_{rel} in kcal/mol. [b] Calculated using eq 1, see text.

becomes less. The C−O stretching mode of HCO^+ at the equilibrium geometry (2137 cm^{-1}) is only 12 cm^{-1} higher than for free CO. This result is not an artifact of strong anharmonicity effects due to frequency calculations carried out at nonequilibrium geometries. Rather, the relatively low C−O stretching frequency of HCO^+ is caused by strong coupling of the C−O mode with the C−H stretching mode. This has been shown before. Goldmann and Krogh-Jespersen calculated the vibrational spectrum of HCO^+, where the proton has an artifically increased mass of 500 au, which reduces the coupling of the two stretching modes significantly.[15] The calculated value for the C−O stretching frequency at the equilibrium geometry was 2369 cm^{-1}. These authors also calculated the harmonic C−O stretching frequency of HCO^+ using the force constant F_{CO} obtained from eq 1. This gives a hypothetical C−O stretching frequency of 2248 cm^{-1}.[15] It follows that the C−O stretching frequency of HCO^+ given by experiment or by direct calculations is not a specific indicator for the C−O bond, because it is significantly influenced by coupling with the C−H mode.[29] Although the effect of mode coupling will be smaller in metal carbonyls, due to the mass of the metals being higher than hydrogen, it becomes clear that the C−O stretching frequency should be used with caution when the electronic structure of the X−CO bond is discussed. A more reliable indicator is the C−O bond distance. Since the trend of the C−O distance can be calculated quite accurately, we will focus in the following on the CO bond length.

In order to investigate the role of the positive charge upon the C−O bond interactions further, we calculated the changes of the bond length, C−O stretching frequency, and force constant of CO when a proton or a positive charge Q^+ approaches CO from the oxygen end. The results are shown in Table 2 and Figures 3 and 4.

The energy curves displayed in Figure 3 show that the well depth of COQ^+ at the equilibrium distance $r_{CO-Q^+} = 1.055$ Å ($D_e = 49.8$ kcal/mol) is slightly less than half of the stabilization energy of COH^+ ($D_e = 102.3$ kcal/mol at $r_{CO-H^+} = 1.007$ Å). The two curves are similar to those calculated for HCO^+ and QCO^+ (Figure 1), except that the stabilization energies are higher for the C-coordinated species. It follows that also for the $CO-H^+$ bond ∼50% of the bonding energy is due to electrostatic effects and that ∼50% are covalent interactions. The covalent contributions arise from the orbital interactions between the HOMO of CO and the empty 1s AO of H^+. Since the HOMO of CO is more localized at the carbon end than at oxygen, HCO^+ is lower in energy than COH^+.

More interesting than the enery change along the reaction coordinate are the changes in the C−O distance. Figure 4 shows that the C−O bond length *increases* when a proton or a positive charge approaches CO from the oxygen end. Only at short distances $CO-H^+$ and $CO-Q^+$ does the C−O bond length become smaller again. At the equilibrium distance $CO-H^+$ (1.007 Å), the C−O bond lengthening ($\Delta r_{C-O} = +0.018$ Å) is nearly the same as calculated for COQ^+ at $r_{O-Q} = 1.007$ Å ($\Delta r_{C-O} = +0.019$ Å; Table 2). It follows that also for COH^+ the effect of the proton upon the C−O bond length is caused by electrostatic effects. *If the HOMO of CO would be antibonding, the C−O bond length of COH^+ should also be shorter than in free CO.* One might argue that the proton in COH^+ interacts more with a lower-lying orbital of CO than with the HOMO, because the HOMO coefficient at the oxygen side is rather small. However, the CO σ-orbital with a large coefficient at oxygen is the lowest lying 3σ valence orbital, which is C−O bonding. It is interesting to note that the C−O stretching frequency and F_{CO} force constant of COH^+ and

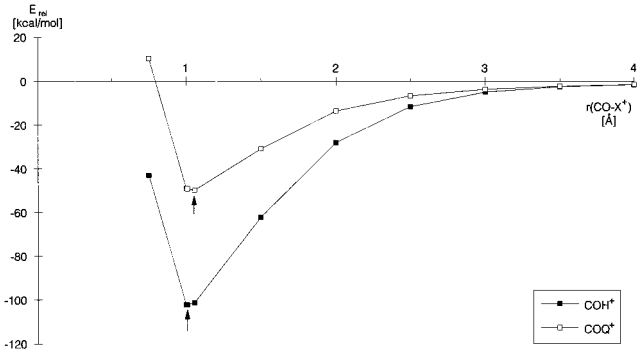

Figure 3. Plot of the calculated energies E_{rel} (kcal/mol) of COX^+ (X = H^+ or point charge Q^+) at various distances $CO-X^+$. Arrows show the position of the equilibrium structure.

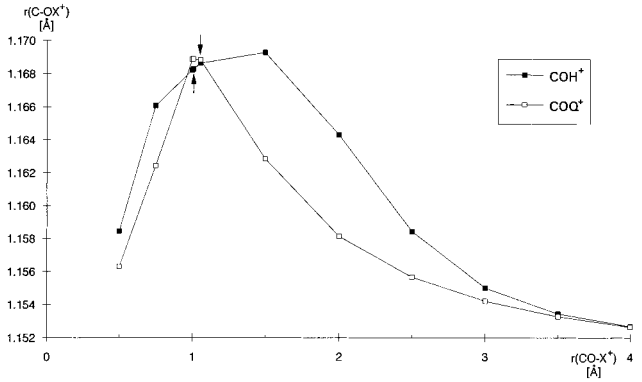

Figure 4. Plot of the calculated C−O distances (Å) of COX^+ (X = H^+ or point charge Q^+) at various distances $CO-X^+$. Arrows show the position of the equilibrium structure.

TABLE 3: Results of the NBO Analysis and the Bader Analysis for the CO Moiety[a]

	NBO					Bader						
molecule	q_C	q_O	q_{CO}	BO	WBI	q_C	q_O	q_{CO}	ρ_b	$\nabla^2\rho_b$	r_b	H_b
CO	0.45	−0.45	0	1.44	2.09	1.18	−1.18	0	3.05	31.97	0.671	−4.99
HCO^+	0.76	−0.09	0.67	1.54	2.35	1.38	−0.87	0.51	3.20	34.94	0.665	−5.47
$(HCO^+)^c$	0.76	−0.09	0.67	1.51	2.34	1.34	−0.83	0.51	3.07	28.32	0.666	−5.25
QCO^+	0.13	−0.13	0	1.52	2.34	1.14	−1.14	0	3.20	35.04	0.666	−5.41
COH^+	0.91	−0.61	0.30	1.24	1.64	1.43	−1.24	0.19	2.64	32.45	0.672	−3.95
COQ^+	0.86	−0.86	0	1.25	1.68	1.57	−1.57	0	2.69	30.11	0.672	−4.08
$LiCO^+$	0.31	−0.28	0.03	1.49	2.22	1.06	−1.03	0.03	3.12	32.08	0.669	−5.22
$CuCO^+$ [b]	0.30	−0.23	0.07	1.51	2.23	1.13	−0.99	0.14	3.14	30.53	0.668	−5.31
$AgCO^+$	0.31	−0.26	0.05	1.51	2.23	1.16	−1.02	0.14	3.13	31.94	0.669	−5.14
$AuCO^+$	0.37	−0.21	0.16	1.52	2.22	1.22	−0.97	0.25	3.13	30.89	0.668	−5.31

[a] q, atomic partial charges. [b] Bader charges with core density added; BO, overlap-weighted NAO bond order; WBI, Wiberg bond index; ρ_b, electron density at the bond critical point in e Å^{-3}; $\nabla^2\rho_b$, Laplacian at the bond critical point in e Å^{-5}; r_b, position of the bond critical point given by the ratio r_{b-O}/r_{C-O}; H_b, energy density at the bond critical point in hartrees Å^{-3}. [c] Calculated using the bond length of free CO (1.151 Å).

COQ^+ decrease when the C−O bond becomes longer, and they increase again when the C−O bond becomes shorter (Table 2). However, the dramatic lowering of the force constant F_{CO} at short distances H^+−CO and Q^+−CO indicate the significant mode coupling with the CO−H^+ and CO−Q^+ stretching vibration.

It is illuminating to analyze the alteration in the *electronic structure* of CO when H^+ or Q^+ approaches the molecule from the carbon or oxygen end. Table 3 shows the calculated atomic partial charges for CO, HCO^+, QCO^+, COH^+, and COQ^+. Because the partitioning of the electronic charge of a molecule on the atoms is dependent on the method, we calculated the atomic charges using two different partitioning schemes, i.e., the NBO method[23] and the topological analysis of the charge distribution.[24] Although the absolute values are clearly different, the changes in the charges at carbon and oxygen resulting from protonation or point charge addition are the same. Both methods predict that, in CO, carbon has a positive charge and oxygen has a negative charge, which leads to electrostatic attraction between the two atoms.[30] The charge separation between C and O *decreases* when a proton or a positive charge Q^+ is attached to the carbon end. This is reasonable, because the positive charge attached to the carbon atom strengthens its electron attraction (increase of the effective electronegativity), which leads to a charge flow from the oxygen atom. It follows that the shortening of the C−O bond in HCO^+ and QCO^+ cannot be explained by the change in the electrostatic interactions between carbon and oxygen. The same conclusion can be made from the calculated charges of COH^+ and COQ^+ (Table 4). The attachment of H^+ or Q^+ to the oxygen atom increases the electron attraction of oxygen, which leads to a higher negative charge at O and a more positive charge at C. If the electrostatic attraction between oxygen and carbon would be the dominant factor for the alteration in the C−O bond lengths, COH^+ and COQ^+ should have a *shorter* C−O bond and HCO^+ and QCO^+ should have a *longer* C−O bond than free CO. Then what is the reason for the calculated changes in the C−O bond lengths?

The answer is given by the calculated changes in the covalent contribution to the bonding between oxygen and carbon. More specifically, the change in the polarization of the molecular orbitals of CO explains the calculated C−O bond shortening of HCO^+ and QCO^+ and the bond lengthening of COH^+ and COQ^+. Table 4 shows the natural localized orbitals (NLMOs) of the calculated compounds.[32] There are two bonding orbitals for CO, one σ orbital and one degenerate π orbital. Both orbitals are strongly polarized toward the oxygen end. The σ orbital has a distribution of 27(C):73(O), and the π orbital has 24(C):76(O). There are also two lone-pair orbitals at C and O,

TABLE 4: NLMO Analysis of the Valence Orbitals at MP2/6-31G(d)[a]

molecule	bond	occ	pol	hybr(C)	hybr(O)
CO	CO(σ)	1.98	27:73	24:75:0.5	44:55:0.7
	CO(π)	1.95	24:76	0:99:0.7	0:100:0.4
	CO(π)	1.95	24:76	0:99:0.7	0:100:0.4
	C(LP)	1.97		78:22:0.0	
	O(LP)	1.98			56:44:0.1
HCO^+	CO(σ)	1.98	32:68	42:58:0.2	40:60:0.6
	CO(π)	1.94	30:70	0:100:0.5	0:100:0.5
	CO(π)	1.94	30:70	0:100:0.5	0:100:0.5
	HC(σ)	1.98	33:67	59:41:0.1	
	O(LP)	1.98			60:40:0.1
$(HCO^+)^b$	CO(σ)	1.97	32:68	42:58:0.2	38:61:0.5
	CO(π)	1.93	30:70	0:100:0.4	0:100:0.5
	CO(π)	1.93	30:70	0:100:0.4	0:100:0.5
	HC(σ)	1.98	33:67	60:40:0.1	
	O(LP)	1.98			62:38:0.1
QCO^+	CO(σ)	1.98	31:69	39:61:0.3	42:57:0.7
	CO(π)	1.94	30:70	0:100:0.4	0:100:0.5
	CO(π)	1.94	30:70	0:100:0.4	0:100:0.5
	C(LP)	1.98		60:40:0.2	
	O(LP)	1.98			58:42:0.1
COH^+	CO(σ)	1.98	22:78	20:80:0.7	55:45:0.3
	CO(π)	1.96	15:85	0:99:1.2	0:100:0.1
	CO(π)	1.96	15:85	0:99:1.2	0:100:0.1
	C(LP)	1.97		82:18:0.0	
	OH(σ)	1.98	86:14		45:55:0.1
COQ^+	CO(σ)	1.98	23:77	21:79:0.7	53:47:0.3
	CO(π)	1.96	16:84	0:99:1.1	0:100:0.1
	CO(π)	1.96	16:84	0:99:1.1	0:100:0.1
	C(LP)	1.97		82:18:0.0	
	O(LP)	1.98			46:54:0.2

[a] occ, occupancy; pol, % of occ, assigned to first and second atom; hybr, % s, p, and d character of the hybrid orbitals; all delocalizations to other atoms are below 0.6%. [b] Calculated using the CO bond length of free CO (1.151 Å).

respectively. The polarization of the bonding orbitals changes significantly when H^+ or Q^+ are attached. The C−O bonding orbitals become *less* polarized[39] in HCO^+ (σ-orbital 32(C):68(O); π-orbital 30(C):70(O)) and in QCO^+ (σ-orbital 31(C):69(O); π-orbital 30(C):70(O)), while they are *more* polarized in COH^+ ((σ-orbital 22(C):78(O); π-orbital 15(C):85(O)) and COQ^+ (σ-orbital 23(C):77(O); π-orbital: 16(C):84(O)). It is interesting to note that the polarization of the π-orbital changes more than the σ-orbital. This is reasonable, because the π bond is higher in energy than the σ bond.

It might be argued that the change in the bond polarization of CO is caused by the shorter C−O bond in HCO^+ rather than the electrostatic effect of the proton and that the discussion uses a chicken-and-egg argumentation. In order to investigate this point, we calculated the electronic structure of HCO^+ using the theoretically predicted C−O bond length of free CO (1.151 Å).

TABLE 5: Theoretically Predicted (CCSD(T)//MP2) and Experimentally Observed Physical Constants of $M(CO)^+$ [a]

	calc					exp	
M^+	r_{M-CO}	r_{MC-O}	D_e (D_0)	ν_{CO}	$\Delta\nu_{CO}$[b]	D_0[c]	$\Delta\nu_{CO}$[b]
Li^+	2.233	1.143	17.9 (16.7)	2176	+58		
Cu^+	1.891	1.142	32.3 (30.9)	2182	+63	36(2)	+35[d]
Ag^+	2.249	1.142	21.8 (20.8)	2181	+59	21(1)	+65[e]
Au^+	1.976	1.142	38.3 (36.9)	2177	+59		+53[f]

[a] Bond lengths r in Å, dissociation energies D in kcal/mol, and vibrational frequencies ν in cm^{-1}. [b] With respect to free CO. [c] Reference 35. [d] Value for $[Cu(CO)](AsF_6)$, ref 6b. [e] Reference 6c. [f] Reference 5f.

Table 3 shows that C−O bond order is nearly the same in (HCO^+), which has r_{C-O} = 1.151 Å, and optimized HCO^+. Table 4 shows that the polarization of the C−O bond orbitals of (HCO^+) is the same as in HCO^+. This shows clearly that the driving force for the C−O bond shortening in HCO^+ is the electrostatically induced change of the polarization of the C−O bond orbitals.

We want to point out that the alteration in the bond polarization of QCO^+ and COQ^+ is very similar to HCO^+ and COH^+, respectively. This supports the conclusion that the effect of attaching a proton to CO is mainly due to electrostatic interactions. The electrostatic interactions play a paradoxical role, however, because they become manifest only indirectly. The electrostatic interactions lead to an opposite change in the polarization of the bonding orbitals of HCO^+ and QCO^+ compared to COH^+ and COQ^+, and thereby to a change in the covalent part of the C−O bonding. *This is the central mechanism which leads to the shortening and lengthening of the C−O bond in HCO^+ and COH^+, respectively.* The change in the hybridization and the C−O bond orders support the above conclusions. The %s character at the carbon end of the C−O σ bond increases in HCO^+ and QCO^+, while it decreases in COH^+ and COQ^+ (Table 4). The C−O bond orders in HCO^+ and QCO^+ are higher than in CO, while they are lower in COH^+ and COQ^+. *It is the change in the covalent contribution to the C−O bond which leads to a shorter or longer bond in the C- and O-protonated isomers.* A more covalent C−O bonding in HCO^+ and QCO^+ and less covalent character in COH^+ and COQ^+ than in CO is also given by the topological analysis of the electron density distribution (Table 3). The electron density at the CO bond critical points of HCO^+ and QCO^+ is higher than in CO, while it is lower in COH^+ and COQ^+. An accumulation of electronic charge has been suggested as indicator of covalent bonding.[33] Another sign for more covalent character in the C−O bonds of HCO^+ and QCO^+ and less covalent bonding in COH^+ and COQ^+ is the calculated energy densities at the bond critical point, which are more negative in the former compounds and less negative in the latter species than in CO.[34]

Interaction of CO with Positively Charged Metals

In order to investigate the influence of the metal → CO π-back-donation on the C−O bond, we calculated CCSD(T) M^+−CO bond energies (i.e., D_0 values) at MP2 optimized M−C and C−O bond lengths of the cationic monocarbonyls $M(CO)^+$ (M = Li, Cu, Ag, Au). In addition, we also calculated C−O bond distances at the MP2 level of theory, at fixed distances M^+−CO between 4.0 and 1.0 Å (M = Li) or between 4.0 and 1.5 Å (M = Cu, Ag, Au).

Table 5 shows calculated equilibrium M^+−CO and C−O bond lengths, M^+−CO bond energies (D_0), and ν(CO) values for the four $M(CO)^+$ complexes. The CCSD(T)//MP2 bond energy for the Cu^+−CO bond (30.9 kcal/mol) is lower by 3 kcal/mol than the lower limit of the range of the experimental value reported by Armentrout and co-workers (36(2) kcal/mol).[35] A previous theoretical study by Bauschlicher and co-workers[36] gave a bond energy D_0 = 32.0 kcal/mol. Our calculated bond energy for Ag^+−CO (D_0 = 20.8 kcal/mol) is in perfect agreement with Armentrout's experimental value (D_0 = 21(1) kcal/mol).[35] There is no experimentally determined D_0 value for the Au^+−CO bond known to us. Our calculated CCSD(T)//MP2 value is 36.9 kcal/mol, significantly lower than the QCISD(T)//MP2 value of 43.5 kcal/mol.[37] We believe that the present value is more reliable, because the CCSD(T) level has been found to give more accurate energies than QCISD(T).[38] Nevertheless, note that the QCISD(T) D_0 value for Ag^+−CO was reported to be 19.7 kcal/mol,[37] virtually the same as the CCSD(T) value of 20.8 kcal/mol.

All four cations $M(CO)^+$ are predicted to have higher C−O stretching frequencies than free CO, the simplest possible hallmark of nonclassical metal carbonyls.[9] Unfortunately, there are no experimental gas-phase vibrational data for free $M(CO)^+$ cations, and it has been shown that the counteranion has a measurable effect on ν(CO). For example, ν(CO) for $[Ag(CO)][OTeF_5]$, $[Ag(CO)][B(OTeF_5)_4]$, and $[Ag(CO)][Nb(OTeF_5)_6]$ are 2189, 2204, and 2208 cm^{-1}, respectively.[6a] Nevertheless, and with this caveat in mind, a comparison of our theoretical ν(CO) values with experimental data will be made. The experimental ν(CO) values in Table 5 are for $M(CO)^+$ salts of the most weakly coordinating anion available for each cation: AsF_6^- for $Cu(CO)^+$, $B(OTeF_5)_4^-$ for $Ag(CO)^+$, and SO_3F^- for $Au(CO)^+$. The MP2 calculations for $Cu(CO)^+$ correctly predict that ν(CO) is higher than in CO, but the calculated frequency shift is much higher (+63 cm^{-1}) than the experimental value (+35 cm^{-1}).[6a] However, calculated ν(CO) values for $Ag(CO)^+$ and $Au(CO)^+$, which are both +59 cm^{-1}, are in excellent agreement with the experimental values of +65 and +53 cm^{-1}, respectively.[6a] It seems possible that ν(CO) values of $Cu(CO)^+$ salts are more counterion dependent than for $Ag(CO)^+$ or $Au(CO)^+$ salts, and we intend to explore this possibility both experimentally and theoretically in the future.

Figure 5 shows plots of MP2-calculated C−O distances as a function of r_{M-CO}. We begin the discussion with Li^+-CO (Figure 5a), which can have no metal → CO π-back-donation. Our results indicate a shortening of the C−O bond length up to r_{Li-CO} = 1.75 Å, which is considerably shorter than the equilibrium bond length of 2.233 Å. At this point an interaction between the filled $1s^2$ core orbital of Li^+ and the lowest lying empty π^* orbital of CO becomes significant, and this leads to a lengthening of the C−O bond. The CDA results shown in Table 6 indicate that the onset of the Li^+ → CO σ-back-donation starts at $r_{Li-CO} \sim 1.50$ Å, while at longer Li^+−CO distances only OC → Li^+ σ-donation is important. It is a significant finding that the M → CO σ-back-bonding can have as large an effect on r_{CO}, and presumably ν(CO), as π-back-bonding does for classical metal carbonyls, even if the effect of σ-back-bonding only occurs at unrealistically short M^+−CO distances.

The plots for $Cu(CO)^+$, $Ag(CO)^+$, and $Au(CO)^+$ (Figure 5, b, c, and d, respectively) have turning points for Δr_{CO} at nearly the same $metal^+$−CO distance of ~2.15 Å. This is a remarkable result, because the three metal cations have quite different equilibrium M^+−CO distances (see Table 5). The M^+−CO equilibrium bond distances of $Cu(CO)^+$ and $Au(CO)^+$ are *shorter* than the turning point of Δr_{CO}, while the equilibrium Ag^+−CO distance is *longer* than the turning point. Nevertheless, the *shortening* of the C−O bond at the equilibrium

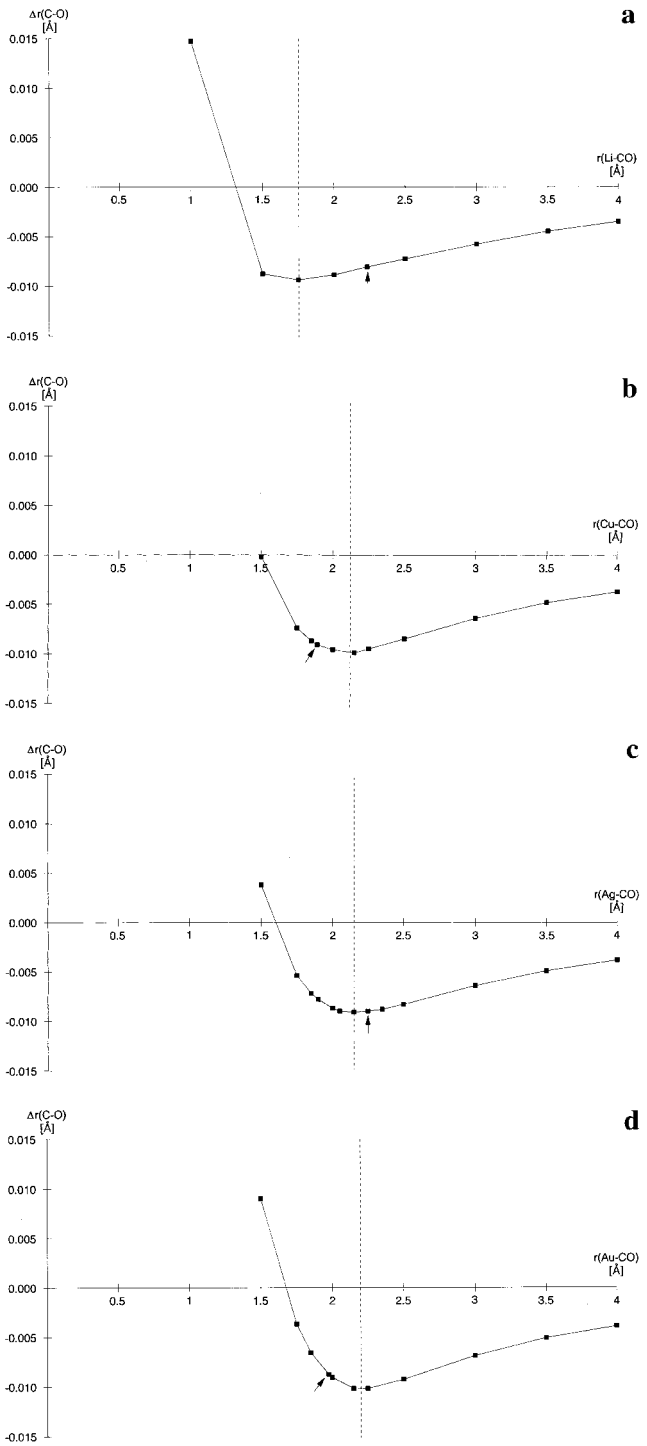

Figure 5. Plot of the calculated C−O distances (Å) of MCO^+ at various distances M^+-CO. (a) M = Li^+; (b) M = Cu^+; (c) M = Ag^+; (d) M = Au^+. Arrows show the position of the equilibrium structure. A dashed line indicates the lowest lying point of the curve.

geometry is nearly the same for the three M^+CO species (0.0091 Å for $Cu(CO)^+$, 0.0089 Å for $Ag(CO)^+$, and 0.0088 Å for $Au(CO)^+$).

Table 3 shows the results of the NBO and topological analysis of the electron density distribution for the $M(CO)^+$ cations at the equilibrium geometries. As expected, there is only a small donation of negative charge from CO to the M^+ cations; the equilibrium metal charges in the $M(CO)^+$ complexes are 0.97, 0.93, 0.95, and 0.84 for Li, Cu, Ag, and Au, respectively. The C−O bond orders and the electron densities at the C−O bond critical point of the $M(CO)^+$ complexes are higher, and the energy density H_b is more negative than in the free CO molecule.

TABLE 6: CDA Results for the OC → M^+ Donation *d*, M^+ → CO Back-donation *b*, and M^+ ↔ CO Repulsive Polarization *r* of $M(CO)^+$ at Various Distances r_{M^+-CO} (Å) at the MP2 Level

M^+	r_{M^+-CO}	*d*	*b*	*r*
Li^+	1.00	0.718	0.065	−0.395
Li^+	1.50	0.541	0.008	−0.098
Li^+	2.00	0.369	0.002	−0.016
Li^+	2.233[a]	0.323	0.001	−0.006
Li^+	2.50	0.276	0.000	−0.002
Li^+	3.00	0.166	0.000	0.000
Li^+	3.00	0.166	0.000	0.000
Li^+	3.50	0.103	0.000	0.000
Li^+	4.00	0.066	0.000	0.000
Cu^+	1.50	0.436	0.228	−0.186
Cu^+	1.75	0.535	0.100	−0.068
Cu^+	1.891[a]	0.537	0.060	−0.047
Cu^+	2.00	0.500	0.036	−0.034
Cu^+	2.15	0.447	0.019	−0.025
Cu^+	2.25	0.408	0.012	−0.021
Cu^+	2.50	0.322	0.004	−0.013
Cu^+	3.00	0.206	0.001	−0.005
Cu^+	3.50	0.135	0.000	−0.003
Cu^+	4.00	0.087	0.000	0.000
Ag^+	1.50	0.549	0.413	−0.443
Ag^+	1.75	0.453	0.161	−0.259
Ag^+	1.85	0.417	0.105	−0.205
Ag^+	2.00	0.380	0.055	−0.147
Ag^+	2.05	0.361	0.040	−0.126
Ag^+	2.15	0.342	0.024	−0.099
Ag^+	2.249[a]	0.327	0.013	−0.077
Ag^+	2.35	0.314	0.009	−0.060
Ag^+	2.50	0.302	0.002	−0.042
Ag^+	3.00	0.235	0.000	−0.010
Ag^+	3.50	0.166	0.000	−0.002
Ag^+	4.00	0.112	0.000	0.000
Au^+	1.50	0.538	0.541	−0.318
Au^+	1.75	0.486	0.246	−0.202
Au^+	1.85	0.452	0.171	−0.166
Au^+	1.976[a]	0.425	0.109	−0.133
Au^+	2.00	0.413	0.094	−0.122
Au^+	2.15	0.387	0.049	−0.090
Au^+	2.25	0.374	0.031	−0.074
Au^+	2.50	0.338	0.008	−0.045
Au^+	3.00	0.243	−0.001	−0.014
Au^+	3.50	0.166	0.000	−0.003
Au^+	4.00	0.116	0.000	0.000

[a] Equilibrium distance.

The result is that the C−O bonds in the four $M(CO)^+$ species are actually more covalent, and correspondingly less ionic, than the C−O bond of free CO.

The CDA results for $M(CO)^+$, listed in Table 6, shed further light on the nature of the M^+−CO bonds. At the M^+−CO equilibrium distances there is significant Au^+ → CO π-back-donation, some Cu^+ → CO π-back-donation, but negligible Ag^+ → CO π-back-donation. Note that the absolute numbers of the calculated charge donation have little meaning; it is the *ratio* of the two donor−acceptor components that is significant. The ratio is 0.11 for $Cu(CO)^+$, 0.04 for $Ag(CO)^+$, and 0.26 for $Au(CO)^+$. The negligible amount of Ag^+ → CO π-back-donation at the Ag−C equilibrium distance is in harmony with our observation that a further shortening of the Ag^+−CO distance results in a slight shortening of the C−O bond, before it results in C−O bond lengthening (see Figure 5c). Table 6 clearly indicates that even a relatively small amount of M^+ → CO π-back-donation is sufficient to lengthen the C−O bond in $M(CO)^+$ complexes.

The differences in $M(CO)^+$ equilibrium bond distances and in the back-donation/donation ratios for M = Cu^+, Ag^+, and Au^+ of $M(CO)^+$ can be understood by examining the radii of their valence s and d orbitals. Since the electronic ground state

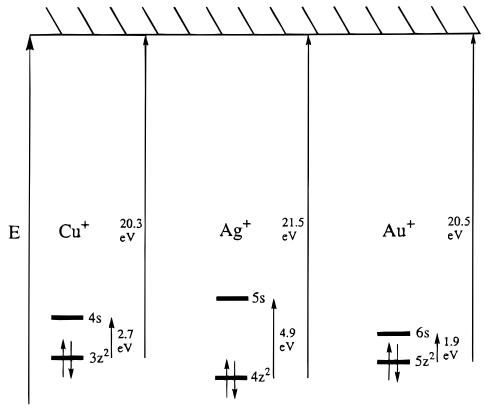

Figure 6. Orbital energy diagram for the highest occupied and lowest unoccupied atomic orbitals of Cu^+, Ag^+, and Au^+ in their ^1S ground state. The d subshell energies correspond to the second ionization potentials for the neutral atoms. The s−d energy gaps correspond to the lowest energy $d^9s^1 \leftarrow d^{10}$ electronic transition energies for the gas-phase M^+ cations.[9]

for these three metal ions is $d^{10}s^0$, the s valence orbital serves as the acceptor orbital and two of the valence d orbitals are the donor orbitals. The radius of the 6s orbital of gold, 3.061 au, is rather small, while the 5d orbital has a comparatively larger radius of 1.618 au[40] The radial expansion of the 5d orbital and the contraction of the 6s orbital are well-known relativistic effects, which are particularly strong for Au.[41] This means that a ligand, L, has to come rather close to the gold cation in order to achieve efficient L → Au^+ σ-donation, and the necessarily short Au^+−L distance leads to significant Au^+ → ligand π-back-donation. In contrast, the 5s orbital of silver has a much larger radius, 3.451 au, than the 6s orbital of gold, while the 4d orbital of Ag has a smaller radius, 1.396 au, than the 5d orbital of Au.[40] It follows that L → Ag^+ σ-donation becomes effective at a distance too long to allow for appreciable π-back-donation. This explains why $Ag(CO)^+$ has a rather long silver−carbon bond with primarily σ-donation and negligible π-back-donation.

Copper is intermediate between silver and gold. The radius of the 4s orbitals of copper is smaller, 3.262 au, than the radius of the 5s orbital of silver, but larger than the radius of the 6s orbital of gold.[40] The radii of the 3d orbitals of the first transition metal row are small because there is no lower-lying shell of d electrons which would yield strong Pauli repulsion. Accordingly, the radius of the 3d orbital of Cu is only 1.002 au.[40] It follows that a ligand can come rather close to Cu^+ before repulsive interactions between the filled σ-donor orbital and the 3d electrons become significant. This leads to a relatively short and strong equilibrium Cu^+−CO bond, and the short bond results in significant π-overlap and hence appreciable Cu^+ → CO π-back-donation.

The orbital energies of the metal cations M^+, shown in Figure 6, are also important for a complete understanding of the metal−carbon bonds. The interaction of the filled CO σ-donor orbital with the filled metal $z^2(d_\sigma)M^+$ atomic orbital leads to σ-repulsion. In general, sd_σ mixing for d^{10} metal ions results in a shift of electron density from the *z* axis (the metal−ligand axis) to the *xy* plane, decreasing the σ-repulsion and allowing for shorter, stronger metal−ligand σ-bonds.[42] The $s-d_\sigma$ energy gaps[43] and d-subshell energy levels for Cu^+, Ag^+, and Au^+ are depicted in Figure 6 (the d-subshell energies correspond to the second ionization potentials of the neutral atoms). The Ag^+ ion, with the largest $s-d_\sigma$ energy gap, forms the weakest metal−ligand bond, while the Au^+ ion, with the smallest energy gap, forms the strongest.

Since π-back-donation involves a shift of electron density from filled metal d-orbitals to empty CO orbitals, it is related to removal of electron density from the metal and hence should be related to ionization potentials. The second ionization potentials of silver (21.5 eV) is larger by ca. 25 kcal/mol than those for copper (20.3 eV) and gold (20.5 eV). In fact, silver has the highest second ionization potential of all metallic elements except for the alkali elements. It is now straightforward to understand why there is negligible π-back-donation in the $Ag(CO)^+$ complex. Since metal → CO π-back-donation has been found to be more important for the metal−CO bond strength than OC → metal σ-donation,[2] it becomes understandable why the Ag^+−CO bond is clearly weaker than the Cu^+−CO and Au^+−CO bonds. The Ag^+ cation has two strikes against it: σ-repulsion leads to a long Ag^+−CO bond distance and poor π-overlap *and* the second ionization potential for silver are too high for effective transfer of electron density from the metal to the CO ligand.

Summary and Conclusion

The shortening of the C−O bond length in HCO^+ and the lengthening in COH^+ relative to free CO are caused by the change in the polarization of the bond orbitals due to the positive charge of the H^+ ion. The bonding orbitals of free CO are polarized toward the oxygen atom because oxygen is more electronegative than carbon. Placing a proton *or* a positive charge at the carbon atom of CO serves to attract electron density from the oxygen atom to the carbon atom, which leads to less polarized σ- and π-bonds and to a more covalent C−O bond in the HCO^+ molecular ion than in free CO. Placing a proton or a positive charge at the oxygen atom has the opposite effect.

The C−O bond distance of $M(CO)^+$ complexes, $M^+ = Li^+$, Cu^+, Ag^+, and Au^+, becomes shorter as the CO molecule approaches M^+ from infinity, but there is a turning point in the vicinity of the equilibrium M^+−CO distance after which the C−O bond begins to lengthen as the M^+−CO distance continues to decrease. The turning point is shorter than the equilibrium M^+−CO distance for Li^+ and Ag^+, but longer than the equilibrium M^+−CO distance for Cu^+ and Au^+. The CDA results show that the lengthening of the C−O bond is caused by the onset of M^+ → CO σ- or π-back-donation. Furthermore, a relatively small amount of M^+ → CO back-donation is sufficient to lengthen the CO bond. The different M^+−CO bond energies and metal−carbon back-donation/donation ratios can be understood in terms of the radial extension and the energies of the valence *n*s and $(n-1)$d orbitals of Cu^+, Ag^+, and Au^+.

Acknowledgment. This work was supported by the Deutsche Forschungsgemeinschaft (SFB 260 and Graduiertenkolleg Metallorganische Chemie) and by the Fonds der Chemischen Industrie. We acknowledge excellent service and generous allotment of computer time of the HRZ Marburg, HHLRZ Darmstadt, and the HLRZ Jülich.

References and Notes

(1) (a) Elschenbroich, C.; Salzer, A. *Organometallics*; VCH: New York, 1992. (b) Cotton, F. A.; Wilkinson, G. *Advanced Inorganic Chemistry*; Wiley: New York, 1980. (c) Gerloch, M.; Constable, E. C. *Transition Metal Chemistry*; VCH: New York, 1994. (d) Constable, E. C. *Metals and Ligand Reactivity*; VCH: New York, 1996.

(2) Davidson, E. R.; Kunze, K. L.; Machado, F. B. C.; Chakravorty, S. J. *Acc. Chem. Res* **1993**, *26*, 628, and further references cited in this work.

(3) (a) Sherwood, D. E.; Hall, M. B. *Inorg. Chem.* **1983**, *22*, 93. (b) Williamson, R. L.; Hall, M. B. *Int. J. Quantum Chem.* **1987**, *21S*, 503. (c) Li, J.; Schreckenbach, G.; Ziegler, T. *J. Am. Chem. Soc.* **1995**, *117*, 486. (d) Ziegler, T.; Tschinke, V.; Ursenbach, C. *J. Am. Chem. Soc.* **1987**, *109*, 4825. (e) Blomberg, M. R. A.; Siegbahn, P. E. M.; Lee, T. L.; Rendell, A. P.; Rice, J. E. *J. Chem. Phys.* **1991**, *95*, 5898.

(4) (a) Dapprich, S.; Frenking, G. *J. Phys. Chem.* **1995**, *99*, 9352. (b) Ehlers, A. W.; Dapprich, S.; Vyboishchikov, F. S.; Frenking, G. *Organometallics* **1996**, *15*, 105.

(5) (a) Selg, P.; Brintzinger, H. H.; Andersen, R. A.; Horváth, I. T. *Angew. Chem.* **1995**, *107*, 877; *Angew. Chem., Int. Ed. Engl.* **1995**, *34*, 791. (b) Guo, Z.; Swenson, D. C.; Guram, A. S.; Jordan, R. F. *Organometallics* **1994**, *13*, 766. (c) Hwang, G.; Wang, C.; Aubke, F.; Willner, H.; Bodenbinder, M. *Can. J. Chem.* **1993**, *71*, 1532. (d) Willner, H.; Bodenbinder, M.; Wang, C.; Aubke, F. *J. Chem. Soc., Chem. Commun.* **1994**, 1189. (e) Aubke, F.; Wang, C. *Coord. Chem. Rev.* **1994**, *137*, 483. (f) Willner, H.; Aubke, F. *Inorg. Chem.* **1990**, *29*, 2195.

(6) (a) Hurlburt, P. K.; Rack, J. J.; Luck, J. S.; Dec, S. F.; Webb, J. D.; Anderson, O. P.; Strauss, S. H. *J. Am. Chem. Soc.* **1994**, *116*, 10003. (b) Rack, J. J.; Webb, J. D.; Strauss, S. H. *Inorg. Chem.* **1996**, *35*, 277. (c) Hurlburt, P. K.; Anderson, O. P.; Strauss, S. H. *J. Am. Chem. Soc.* **1991**, *113*, 6277.

(7) Bach, C.; Willner, H.; Wang, C.; Rettig, S. J.; Trotter, J.; Aubke, F. *Angew. Chem.* **1996**, *108*, 2104; *Angew. Chem., Int. Ed. Engl.* **1996**, *35*, 1974.

(8) (a) Szilagyi, R.; Frenking, G. *Organometallics* **1997**, *16*, 4807. (b) Lupinetti, A.; Frenking, G.; Strauss, S., to be published.

(9) Strauss, S. H. *Chemtracts-Inorg. Chem.* **1997**, *10*, 77.

(10) (a) Reference 1a. (b) Albright, T. A.; Burdett, J. K.; Whangbo, M. H. *Orbital Interactions in Chemistry*; Wiley: New York, 1985.

(11) DeKock, R. L.; Sarapu, A. C.; Fenske, R. F. *Inorg. Chem.* **1971**, *10*, 38.

(12) Herzberg, G. *Molecular Spectra and Molecular Structure. Volume I—Spectra of Diatomic Molecules*; Krieger Publishing Co.; Malabar, 1989.

(13) Hirota, E.; Endo. J. *J. Mol. Spectrosc.* **1988**, *127*, 524.

(14) (a) Woods, R. C. *Philos. Trans. R. Soc.* **1988**, *A324*, 141. (b) Woods, R. C., private communication, in: Berry, R. J.; Harmony, M. D. *J. Mol. Spectrosc.* **1988**, *128*, 176.

(15) Goldman, A. S.; Krogh-Jespersen, K. *J. Am. Chem. Soc.* **1996**, *118*, 12159.

(16) For recent work see: (a) Ferrari, A. M.; Ugliengo, P.; Garrone, E. *J. Chem. Phys.* **1996**, *105*, 4129. (b) Su, Y.-N.; Tsai, M.-S.; Chu, S.-Y. *Int. J. Quantum Chem.* **1996**, *59*, 487. (c) Nandi, P. K.; Sannigrahi, A. B. *J. Mol. Struct. THEOCHEM* **1994**, *113*, 99. (d) Grice, S. T.; Harland, P. W.; Maclagan, R. G. A. R. *J. Chem. Phys.* **1993**, *99*, 7619. (e) Puzzarini, C.; Tarroni, R.; Palmieri, P.; Carter, S.; Dore, L. *Mol. Phys.* **1996**, *87*, 879. (f) Weis, B.; Yamashity, K. *J. Chem. Phys.* **1993**, *99*, 9512. (g) Szulejko, J. E.; McMahon, T. B. *J. Am. Chem. Soc.* **1993**, *115*, 7839. (h) Smith, B. J.; radom, L. *J. Am. Chem. Soc.* **1993**, *115*, 4885. (i) Komornicki, A.; Dixon, D. A. *J. Chem. Phys.* **1992**, *97*, 1087.

(17) Hall, M. B.; Fenske, R. F. *Inorg. Chem.* **1972**, *11*, 1619.

(18) Beach, D. B.; Jolly, W. L. *Inorg. Chem.* **1985**, *24*, 567.

(19) (a) Dolg, M.; Wedig, U.; Stoll, H.; Preuss, H. *J. Chem. Phys.* **1987**, *86*, 866. (b) Andrae, D.; Häussermann, U.; Dolg, M.; Stoll, H.; Preuss, H. *Theor. Chim. Acta* **1990**, *77*, 123.

(20) (a) Cizek, J. *J. Chem. Phys.* **1966**, *45*, 4256. (b) Cizek, J. *Adv. Chem. Phys.* **1966**, *14*, 35. (c) Pople, J. A.; Krishnan, R.; Schlegel, H. B.; Binkley, J. S. *Int. J. Quantum Chem.* **1978**, *14*, 545. (d) Bartlett, R. J.; Purvis, G. D. *Ibid.* **1978**, *14*, 561. (e) Purvis, G. D.; Bartlett, R. J. *J. Chem. Phys.* **1982**, *76*, 1910. (f) Purvis, G. D.; Bartlett, R. J. *Ibid.* **1987**, *86*, 7041.

(21) *Gaussian 94*; Frisch, M. J.; Trucks, G. W.; Schlegel, H. B.; Gill, P. M. W.; Johnson, B. G.; Robb, M. A.; Cheeseman, J. R.; Keith, T. A.; Petersson, G. A.; Montgomery, J. A.; Raghavachari, K.; Al-Laham, M. A.; Zakrzewski, V. G.; Ortiz, J. V.; Foresman, J. B.; Cioslowski, J.; Stefanov, B. B.; Nanayakkara, A.; Challacombe, M.; Peng, C. Y.; Ayala, P. Y.; Chen, W.; Wong, M. W.; Andres, J. L.; Replogle, E. S.; Gomberts, R.; Martin, R. L.; Fox, D. J.; Binkley, J. S.; Defrees, D. J.; Baker, I.; Stewart, J. J. P.; Head-Gordon, M.; Gonzalez, C.; Pople, J. A. Gaussian Inc.: Pittsburgh, PA, 1995.

(22) ACES II, an ab initio program system written by J. F. Stanton, J. Gauss, J. D. Watts, W. J. Lauderdale, and R. J. Bartlett, University of Florida, Gainesville, FL 1991.

(23) Reed, A. E.; Curtiss, L. A.; Weinhold, F. *Chem. Rev.* **1988**, *88*, 899.

(24) Bader, R. F. W. *Atoms in Molecules: A Quantum Theory*; Oxford University Press: Oxford, UK, 1990.

(25) CDA 2.1. Dapprich, S.; Frenking, G. Universität Marburg. The program is accessible under ftp://chemie.uni-marburg.de.

(26) Biegler-König, F. W.; Bader, R. F. W.; Ting-Hua, T. *J. Comput. Chem.* **1982**, *3*, 317.

(27) Martin, J. M. L.; Taylor, P. R.; Lee, T. J. *J. Chem. Phys.* **1993**, *99*, 286.

(28) Adams, N. G.; Smith, D.; Tichy, M.; Javhery, G.; Twiddy, N. D.; Ferguson, E. E. *J. Chem. Phys.* **1989**, *91*, 4037.

(29) This is also obvious by analyzing the components of the calculated C−O stretching mode of HCO^+, which have strong contributions from the movement of the proton.

(30) The reader should not confuse the atomic charge distribution with the dipole moment of CO. Carbon monoxide has a very low dipole moment (0.11 D), with the negative end at the carbon side.[31] The measured dipole moment is the resulting vector along the C−O axis from the 3-dimensional charge distribution, which has a significant concentration at oxygen in the π-region. The charge distribution of the σ-symmetric HOMO of CO, which has its largest extension at the more diffuse carbon end, overcompensates because of its shape the higher charge concentration at the more compact oxygen atom.

(31) Nelson Jr., R. D.; Lide Jr., D. R.; Maryott, A. A. *National Reference Data Series*; NSRDS-NBS 10; National Bureau of Standards: Washington, DC.

(32) The change of the polarization of the molecular orbitals can also be given for the canonical orbitals. The use of localized orbitals facilitates the discussion, because only two orbitals, one σ and one degenerate π orbital need to be considered.

(33) Reference 24, p 290.

(34) Cremer, D.; Kraka, E. *Angew. Chem.* **1984**, *96*, 612; *Angew. Chem., Int. Ed. Engl.* **1984**, *23*, 627.

(35) Meyer, F.; Chen, Y.-M.; Armentrout, P. B. *J. Am. Chem. Soc.* **1995**, *117*, 4071.

(36) Barnes, L. A.; Rosi, M.; Bauschlicher, C. W. Jr. *J. Chem. Phys.* **1990**, *93*, 609.

(37) Veldkamp, A.; Frenking, G. *Organometallics* **1993**, *12*, 4613.

(38) Böhme, M.; Frenking, G. *Chem. Phys. Lett.* **1994**, *224*, 195.

(39) A more even distribution of the bonding π electrons between C and O has been suggested in a qualitative model as the reason for the strengthening of the bond in CO^+: Jaffé, H. H.; Orchin, M. *Tetrahedron* **1960**, *10*, 212.

(40) Desclaux, J. P. *At. Data Nucl. Data Tabl.* **1973**, *12*, 312. The radii have been calculated for M^0, but it can be assumed that the s/d ratios of M^+ do not change significantly.

(41) Pyykkö, P. *Chem. Rev.* **1988**, *88*, 563.

(42) Orgel, L. E. *J. Chem. Soc.* **1958**, 4186.

(43) Moore, C. E., *Atomic Energy Levels*; National Bureau of Standards: Washington, DC, 1971.